Cysteine 343 in the Substrate Binding Domain is the Primary *S*-Nitrosylated Site in Protein Disulfide Isomerase

Jiro Ogura[1,2]*, Lloyd W Ruddock[2]*, and Nariyasu Mano[1]

1 Department of Pharmaceutical Sciences, Tohoku University Hospital, Sendai, Japan
2 Faculty of Biochemistry and Molecular Medicine, University of Oulu, Oulu, Finland

* Correspondence:
Jiro Ogura Ph.D.
Assistant Professor
Department of Pharmaceutical Sciences, Tohoku University Hospital, Sendai, Japan, 1-1 Seiryo-machi, Aoba-ku, Sendai 980-8574, Japan
Phone: +81-22-717-7541
E-mail: jiro.ogura@hosp.tohoku.ac.jp

Lloyd Ruddock Ph.D.
Faculty of Biochemistry and Molecular Medicine, University of Oulu, Aapistie 7, 90220 Oulu, Finland
Phone: +358-294-481683
E-mail: Lloyd.Ruddock@oulu.fi

Authors email addresses
Jiro Ogura: jiro.ogura@hosp.tohoku.ac.jp
Lloyd W Ruddock: Lloyd.Ruddock@oulu.fi
Nariyasu Mano: mano@hosp.tohoku.ac.jp

Author contributions
LWR and NM conceived of and supervised the study; JO designed and performed the experiments; JO analyzed the data; JO and LWR wrote the manuscript; and NM reviewed the manuscript. All authors approved the final version of the manuscript.

Abstract

Abnormal protein accumulations are typical pathological features for neurodegenerative diseases. Protein disulfide isomerase (PDI) is a critical enzyme in oxidative protein folding. *S*-nitrosylated PDI has been detected in the postmortem brain in neurodegenerative disease patients, but the effect of *S*-nitrosylation on PDI function and developing neurodegeneration was not clarified in detail. In this study, we identified that *in vitro* and *in vivo S*-nitrosylation of C343 in the **b'** domain of PDI occurs. Reduced recombinant human PDI (hPDI) reacted quickly with *S*-nitrosocompounds, with an observed increase in the expected *S*-nitrosylated species and the appearance of the disulfide state of the active sites. Both Mononitrosylated and dinitrosylated were observed from the *S*-nitrosylation of hPDI. Dinitrosylated species were *S*-nitrosylated both cysteines at active site. But, at least in part, mononitrosylated species were *S*-nitrosylated on cysteine 343 in the substrate binding **b'** domain. Although active site *S*-nitrosylation is reversible by reduced glutathione, *S*-nitrosylation of C343 is comparative stable. *S*-nitrosylation of PDI in SH-SY5Y cells was observed after the *S*-nitrosocysteine (SNOC) treatment and *S*-nitrosylated PDI was still detected 24 h after removing SNOC. While wild-type PDI was *S*-nitrosylated, the level of *S*-nitrosylation of the C343S mutant in over-expressed cells was substantially lower and only wild-type PDI of *S*-nitrosylation remained 24 h after removing SNOC in over-expressed cells. Both of *in vitro* and *in vivo* results suggested that *S*-nitrosylation of C343 in PDI may be the

causative effect on physiological changes in neurodegerenative disease patients, and may be useful for the drug development for neurodegenerative diseases.

Keywords

Neurodegenerative diseases, Protein disulfide isomerase, Nitrosative stress, *S*-nitrosylation

Abbreviations: Amyotrophic lateral sclerosis (ALS); Dulbecco's Modified Eagle's Medium (DMEM); Electrospray ionization (ESI); Ethylenediaminetetraacetic acid (EDTA); *N*-Ethylmaleimide (NEM); Hanks' Balanced Salt Solution (HBSS); human PDI (hPDI); Immobilized metal ion adsorption chromatography (IMAC); 2-Mercaptoethanol (2-ME); Methylmethanethiosulfonate (MMTS); *S*-nitrosocysteine (SNOC); *S*-nitrosoethanol (SNO-EtOH); *S*-nitrosoglutathione (GSNO); Polyvinylidene fluoride (PVDF); Protein disulfide isomerase (PDI); Radioimmunoprecipitation assay (RIPA); Reduced glutathione (GSH); Tobacco etch virus (TEV); Tris-buffered saline containing 0.1% Tween 20 (TBS-T).

1. Introduction

Neurodegenerative diseases, such as Alzheimer's disease, Parkinson's disease and Amyotrophic lateral sclerosis (ALS), are among the most significant clinical challenges to overcome in 21st century. Since there are no curative drugs at present, neurodegenerative diseases are one of greatest unmet medical needs [1–3]. One of main causes preventing drug development for neurodegenerative disease is that nerve cells cannot regenerate after severe cell damage. Thus, it is important to understand the physiological and/or pathological changes at an early stage of neurodegenerative diseases. Abnormal protein accumulations are typical pathological features for neurodegenerative diseases [4,5], and they can be present before the onset of clinical features, such as cognitive or behavioral disorders [6–8].

Protein disulfide isomerase (PDI) is a critical enzyme for oxidative protein folding in the endoplasmic reticulum. It assists protein folding by acting both a chaperone and as an oxidoreductase [9–13]. PDI has U-shape structure composing four structural domains, **a**, **b**, **b'**, and **a'**, a linker region **x** between the **b'** and **a'** domains, and a C-terminal acidic extension [14]. The **a** and **a'** domains are located at either end of the U-shape and contain the CGHC active site motifs. The cysteines in the active site motif are highly reactive [15–17], and can perform thiol-disulfide exchange reactions. The **b** and **b'** domains are located to the base of the U-shape. The **b'** domain contains the principal non-native protein-binding site [18,19], and is required for isomerization reactions. The function of the **b** domain is probably structural.

There is a known association between PDI and neurodegenerative diseases. Several groups have reported that mutations or modification in PDI family members are associated with the risk of ALS and cause motor dysfunction in ALS [20–23]. Moreover, *S*-nitrosylated PDI was detected in the postmortem brain in various neurodegenerative disease patients, such as Alzheimer's disease patients [24], Parkinson's disease patients [24] and ALS patients [25], though the effects of *S*-nitrosylation on PDI function and developing neurodegeneration were not clarified in detail. Since mutations in the cysteines in the active site motif (CGHC) of PDI cause decreased PDI activity [26], those cysteines were speculated to be *S*-nitrosylation sites [24,25]. Recombinant PDI protein activity was decreased by the reaction with *S*-nitrosocompounds, and PDI overexpression could suppress the accumulation of α-Synuclein in the Parkinson disease neuro cell model [24]. Despite the reversibility of *S*-nitrosylation [27], *S*-nitrosylated PDI was stable enough to be detected in postmortem brain [24,25]. However, the cysteines in the active motif are exposed on the protein surface and endogenous antioxidants, which are able to reduce *S*-nitrosylated protein, should be able to readily access these cysteines [14]. Indeed, reduced glutathione (GSH) can rapidly react with the active site disulfide of PDI [15].

Together these findings indicate that to understand the effect of *S*-nitrosylated PDI on physiological and/or pathological changes during neurodegeneration it is important to identify the *S*-nitrosylation site on PDI. In this study, we demonstrate that upon addition of *S*-

nitrosocompounds, the reduced active sites of PDI are oxidized to the disulfide state unless the *S*-nitrosocompounds are present in large excess whereupon di-S-nitrosylation of the dithiol active site occurs. This is rapidly reversible with reduced glutathione. In contrast, we identify that *in vitro* and *in vivo S*-nitrosylation of C343 in the substrate binding **b'** domain of PDI occurs, and that *S*-nitrosylation of C343 is only slowly reversible by glutathione.

2. Materials and methods

2.1 Chemicals

S-nitrosocysteine (SNOC), *S*-nitrosoglutathione (GSNO), and *S*-nitrosoethanol (SNO-EtOH) were synthesized in our laboratory using previously reported methods [28,29] with some modification (Fig. S1). The concentration of the respective nitrosothiol was determined spectrometrically using extinction coefficients ε_{338} = 900 $M^{-1}cm^{-1}$ and ε_{335} = 920 $M^{-1}cm^{-1}$ for SNOC and GSNO, respectively [29]. The concentration of SNO-EtOH was estimated using extinction coefficients ε_{335} = 920 $M^{-1}cm^{-1}$, because based on the value for the *S*-nitrosothiol group [30–32]. Under these conditions, the yield of each nitrosothiol was more than 95% (Table. S1). All stock solutions were stored at -80°C in the dark, and only minor degradation was observed over 6 months under these storage conditions (Fig. S1D).

2.2 Molecular biology

Expression vectors (Table S2) were prepared using standard molecular techniques, including site-directed mutagenesis with the QuickChange site-directed mutagenesis kit (Stratagene, La Jolla, CA). The gene fragments of PDI wild type [33], PDI **a** domain W128F [15], and PDI **a** domain C56S/W128F [15] were cloned with restriction digestion and ligation into a modified pET23-based vector with a pTac promoter replacing the T7 promoter [34]. The variant used included an in-frame N-terminal His-tag followed by a tobacco etch virus (TEV) protease cleavage site (sequence –MHHHHHHSSGGGTENLYFQGHM–) with the final HM being encoded by an in-frame NdeI site. PDI C312A, PDI C343A and PDI C312A/C343A were prepared from pJO3 which encoded wild-type PDI, by the site-directed mutagenesis. Above mentioned plasmids generated were sequenced (Biocenter Oulu core facility) to ensure that there were no errors in the cloned gene. For establishment of over expressed cell lines, we used the plasmids containing EGFP (VB180912-1349cet), human PDI wild type (VB180911-1011yrt) and PDI C343S (VB180911-1012rpy), and those are pRP with the CMV promoter. Those plasmids were generated by VectorBuilder (Guangzhou, China).

2.3 Preparation of recombinant PDI proteins

Recombinant mature human PDI (hPDI) wild type, hPDI C312A, hPDI C343A, hPDI C312A/C343A, hPDI **a** domain W128F, and hPDI **a** domain C56S/W128F were expressed with a TEV protease-cleavable N-terminal his-tag and prepared as the non-tagged form by TEV

proteolysis. hPDI wild type and cysteine mutants were expressed in BL21 (DE3) cells. hPDI **a** domain mutants were expressed in RV308 cells. The cells were cultivated in EnPressoB (Biosilta Oy, Oulu, Finland) media as instructed by the manufacturer. Pellets were resuspended in 100 ml (the same volume as the culture media) sodium phosphate, pH 7.3, 100 μg/ml egg white lysozyme, and 20 μg/ml DNase and frozen. Cells were lysed by two rounds of freeze–thawing, and purified by immobilized metal ion adsorption chromatography (IMAC) using HiTrap Chelating HP (Amersham Biosciences, Uppsala, Sweden) with $NiCl_2$ as per the manufacturer's instructions. His-tagged proteins were eluted by 50 mM ethylenediaminetetraacetic acid (EDTA). IMAC eluates were buffer-exchanged to 20 mM sodium phosphate, pH 7.4 with Amicon Ultra centrifugal filters (10K) (Merck Millipore, Billerica, MA), and mixed with His-tagged TEV protease. TEV protease–cleaved proteins were loaded to HiTrap Chelating HP loaded with $NiCl_2$. Since the cleaved proteins which lack the his-tag could not bind the column, the proteins were obtained in the flow through. After buffer-exchanging to 20 mM sodium phosphate, pH 7.4 with Amicon Ultra centrifugal filters (10K), TEV protease–cleaved proteins were bound to a 6-ml Resource Q anion exchanger (GE Healthcare, Munich, Germany) pre-equilibrated with the same buffer. PDI was eluted by increasing NaCl from 0 to 1 M in 20 mM sodium phosphate, pH 7.4 for 30 min at 2 mL/min (10 column volumes). Purity was assessed by SDS–PAGE, the purest 1ml fractions were pooled, concentrated by Amicon Ultra centrifugal filters (10K). Protein concentrations were determined

using calculated molecular masses and absorption coefficients at 280 nm.

2.4 Reaction of recombinant PDI with various nitrosocompounds

The reaction was started by adding *S*-nitrosocompound (100 or 500 μM) to reduced hPDI (2 μM), and then incubating in 20 mM sodium phosphate buffer, pH 7.4, for the designated time. The experiment for the stability of nitrosylated species in the presence of GSH was performed as follows: reduced hPDI (2 μM) was reacted with SNOC or GSNO at 500 μM for an hour and then treated for 15 min with 10 mM GSH or a buffer control. To quench the reaction free thiol groups were alkylated by the addition of 37.5 mM *N*-Ethylmaleimide (NEM) and 2 M Urea for 7 min. The alkylation was stopped with 0.5% TFA. The NEM-trapped samples were purified by Pierce™ C18 Spin Columns (Thermo Fisher Scientific, Waltham, MA) and analyzed by electrospray ionization (ESI) mass spectrometry (Synapt G2, Waters, Milford, MA, USA) coupled to ACQUITY UPLC machinery (Waters) with BEH300 C4 1.7 μm 2.1 × 100 mm UPLC column (Waters) for desalting and protein separation prior mass spectrometric analysis. UPLC was performed using 0.4 mL/min flow with 0.1% formic acid and 3% to 70% acetonitrile gradient over 15 min. The sum of peak areas for all PDI species at each time point was set to 100%.

2.5 Cell culture

SH-SY5Y cells obtained from the European Collection of Authenticated Cell Cultures (ECACC; Wiltshire, UK) were maintained in plastic culture dish (TPP, Trasadingen, Switzerland). The medium consisted of Dulbecco's Modified Eagle's Medium (DMEM) (Nacalai Tesque, Kyoto, Japan) supplemented with 10% fetal bovine serum (Gibco, Carlsbad, CA) and 100 IU/mL penicillin-100 mg/mL streptomycin (Nacalai Tesque). The cells were grown in an atmosphere of 5% CO_2–95% air at 37°C.

SH-SY5Y cells were transfected with Lipofectamine 2000 (Invitrogen, Carlsbad, CA) according to the manufacturer’s instruction. After selection in G418 (0.5 mg/mL), PDI wild type and PDI C343S expression was confirmed by Western blotting (see results). Cells transfected with the empty pRP-EGFP vector were used as controls. Cells were grown in DMEM supplemented with 10% fetal bovine serum (Gibco, Invitrogen) and G418 (0.5 mg/mL) at 37°C, 5% CO_2, and 95% air.

SNOC exposure at 100 μM was for 30 min in Hanks' Balanced Salt Solution (HBSS) buffered with 10 mM HEPES, then the media was replaced and the cells incubated in FBS free culture medium for 24 h. The cells were harvested at finishing SNOC exposure (30 min) and 24 h after removing SNOC.

2.6 Western Blotting

Cells were lysed in radioimmunoprecipitation assay (RIPA) buffer (50 mM Tris-HCl

(pH 7.4), 150 mM NaCl, 0.5% sodium deoxycholate, 1.0% Triton-X100, 0.1% SDS, 2 mM EDTA, 10 mM NaF, 1 mM phenylmethylsulfonyl fluoride and Halt™ Protease and Phosphatase Inhibitor Cocktail (Thermo Fisher Scientific)). The protein content of the solubilized cells was determined by the BCA protein assay kit (Thermo Fisher Scientific) with bovine serum albumin as a standard. Twenty micrograms of protein were subjected to SDS-PAGE and then transferred to polyvinylidene fluoride (PVDF) membranes (Bio-Rad Laboratories, Hercules, CA). Blots were blocked by 1 or 3% skim milk in tris-buffered saline (20 mM Tris, 137 mM NaCl, pH 7.6) containing 0.1% Tween 20 (TBS-T) at room temperature for 3 h, and then probed with PDI (C81H6) Rabbit mAb (1:500, #3501, Cell Signaling Technology) or beta Actin Mouse Monoclonal antibody (1:1000 dilution, 60008-1-Ig, Proteintech, Portland, ME) at 4°C overnight. The blots were washed and then incubated with mouse anti-rabbit IgG-HRP (1:2,000 dilution, sc-2357, Santa Cruz Biotechnology, Santa Cruz, CA) or peroxidase-conjugated Affinipure goat anti-mouse IgG+IgM (H+L) secondary antibody (1:2,000 dilution, 115-035-044, Jackson Immunoresearch Laboratories, West Grove, PA). Clarity™ Western ECL Substrate (Bio-Rad Laboratories) was used for detection.

2.7 Biotin Switch Assay

Cell lysates were prepared in lysis buffer (25 mM HEPES, pH7.4, 50 mM NaCl, 0.1 mM EDTA, 1% Triton X-100, 1 mM phenylmethylsulfonyl fluoride and Halt™ Protease

and Phosphatase Inhibitor Cocktail (Thermo Fisher Scientific)). The protein content of the solubilized cells was determined by the BCA protein assay kit (Thermo Fisher Scientific) with bovine serum albumin as a standard. For experiments employing 1 mg of protein, free thiols of samples were blocked by methylmethanethiosulfonate (MMTS). After removing excess MMTS by acetone precipitation, nitrosothiols were then reduced to free thiols by using 20 mM sodium ascorbate. The newly formed thiols were linked to the sulfhydryl-specific biotinylating reagent biotin–HPDP. After removing excess biotin-HPDP by acetone precipitation, the biotinylated proteins were pulled down using streptavidin–agarose beads, and SNO-Protein remaining in the samples was detected by performing western blotting.

3. Results

3.1 Reaction of hPDI with various *S*-nitrosocompounds

While *S*-nitrosylation has been implicated as a contributing factor in activation of the UPR and in neurodegenerative diseases [24,25] including Alzheimer's disease and ALS, it is unclear which cysteine residues in PDI are *S*-nitrosylated. The general assumption is the reactive N-terminal cysteine in the active site CGHC motif will be *S*-nitrosylated and this will have a direct impact on the function of this essential protein folding catalyst (Fig. 1A). However, PDI also has two conserved cysteines in its **b'** domain, which is linked to the ability to bind substrates [18,19]. Hence, *S*-nitrosylation of these cysteines may also impact directly or

indirectly on the function of PDI.

To examine which cysteines become *S*-nitrosylated, we examined the reaction of reduced hPDI with *S*-nitrosocompounds followed by ESI mass spectrometry. As predicted PDI reacted quickly with SNOC and GSNO leading to the rapid disappearance of the fully reduced species (Fig. 1B-C). The second order rate constants for the kinetics of disappearance of reduced PDI were 120 ± 10 $M^{-1}s^{-1}$ for SNOC and 61 ± 7 $M^{-1}s^{-1}$ for GSNO. These are of the same order of magnitude as the reaction of the N-terminal active site cysteine of the isolated **a** domain with oxidized glutathione (188 $M^{-1}s^{-1}$; [15]) and faster than oxidation of the active site dithiol of this domain to a disulfide by dehydroascorbate (12.5 $M^{-1}s^{-1}$; [35]).

3.2 The conversion of reduced hPDI to the disulfide state by *S*-nitrosocompound

The loss of the reduced species of PDI by reaction with SNOC and GSNO was concomitant with both an observed increase in the expected *S*-nitrosylated species and the appearance of up to two disulfide bonds in hPDI (Fig. 1B-C). Most likely these disulfide bonds results from the conversion of the dithiol active sites in the reduced states of PDI being converted to the oxidized state (as found during the normal redox cycle of PDI). This is consistent with the known reactivity and catalytic cycle of PDI [12] as well as the rapid formation of a disulfide in dihydrolipoic acid upon nitrosylation, with the formation of nitrous oxide and hydroxylamine (Fig. 1D; [36,37]).

To confirm that the active sites of PDI can be oxidized to the disulfide state by nitrosylation we examined the reactivity of the isolated reduced catalytic **a** domain of PDI with SNOC and GSNO (Fig. 2A-B). Consistent with the results from full length PDI there was a rapid loss of the reduced species with initial second order rate constants of 87 ± 17 $M^{-1}s^{-1}$ and 63 ± 12 $M^{-1}s^{-1}$ for SNOC and GSNO respectfully. Concomitantly there was also the formation of the disulfide species with initial rate constants of 75 ± 16 $M^{-1}s^{-1}$ and 59 ± 11 $M^{-1}s^{-1}$ for SNOC and GSNO respectfully.

3.3 The production of dinitrosylated hPDI by *S*-nitrosocompounds

If the only product from *S*-nitrosylation of the active sites of PDI is the formation of the oxidized active site, then nitrosylation would not have the reported effects [24,25]. Other products must be formed and it these which must result in the reported biological effects.

Other products were observed from the *S*-nitrosylation of the reduced **a** domain, in particular a small amount of single *S*-nitrosylated species was observed (maximally 9.6% at 15 seconds reaction time) and a dinitrosylated species which reached up to 22% of the total protein (Fig. 2A-B). This dinitrosylation most likely arose from a kinetic competition between the *S*-nitrosylation of the second active site cysteine vs the reaction of this cysteine with the other nitrosylated active site cysteine to form a disulfide bond (Fig. 2C). To confirm that this arose from such kinetic partitioning and not from the reaction of other amino acids in the protein, we

examined the reaction of the C56S mutant of the **a** domain to SNOC and GSNO. This mutant which lacks the C-terminal active site cysteine would be expected to form only single nitrosylated or cysteinylated/glutathionylated species and it does (Fig. 2D and E), indicating that dinitrosylation or disulfide bond formation of either active site of PDI arises from the kinetic partitioning scheme shown in figure 2C.

Dinitrosylation was also observed for full length hPDI (Fig. 1B-C), with up to 33% of the protein exhibiting a dinitrosylated state after 30 min reaction with SNOC, while up to 19% was observed with the slower reacting GSNO. To further confirm that dinitrosylation arose from kinetic partitioning (Fig. 2C) the reaction of hPDI with SNOC or GSNO was repeated at 5x lower concentrations of *S*-nitrocompounds. This resulted in a reduction in the dinitrospecies formed (Fig. S2A-D). As further confirmation the reaction of hPDI with the less reactive SNO-EtOH was undertaken. With SNO-EtOH the second order rate constant for the disappearance of the reduced hPDI was only $2.0 \pm 0.2\ M^{-1}s^{-1}$ and no dinitrosylated species was observed (Fig. 3).

3.4 *S*-nitrosylation of the b' domain of hPDI by *S*-nitrosocompounds

Active site disulfide or dinitrosylated species were not the only species observed. Mono nitrosylated species were also observed (Figs. 1-3). Some of these could be intermediates (Fig. 2C), but the appearance of up to 20% of the total PDI being a state with two disulfides

and one *S*-nitrosylation implies that at least one of the cysteines in the **b'** domain of hPDI is also being *S*-nitrosylated.

To examine which of these two cysteines in hPDI could be *S*-nitrosylated, C312A and C343A forms of hPDI were constructed as well as the double mutant C312A/C343A. Purified proteins were then reacted with SNOC and GSNO and the kinetics monitored by ESI mass spectrometry. Disappearance of the reduced species, and appearance of the disulfide and dinitrosylated states were not affected by the mutations (Fig. 4). In contrast, the two disulfide and one *S*-nitrosylated state was only observed for the wild-type (Fig. 1B-C) and C312A mutant (Fig. 4A-B). It was not observed for the C343A single or C312A/C343A double mutant of hPDI (Fig. 4C-F). This implies that hPDI is *S*-nitrosylated on cysteine 343 in the substrate binding **b'** domain.

In order to attempt to obtain mono-nitrosylated C343 species for functional studies, oxidized PDI was reacted with SNOC and GSNO. No nitrosylation of PDI was observed under any condition. Hence C343 appears to only be exposed for nitrosylation when at least one active site is in the reduced state. This explains the low degree of nitrosylation of C343 (maximally 20% of the final product is the two disulfide one nitrosylation when starting from reduced PDI) and makes *in vitro* elucidation of the consequences of C343 nitrosylation problematic. The accessibility of C343 varying with the redox state of the active sites is consistent with the reported change in structure of PDI upon redox state [38].

3.5 Stability of the *S*-nitrosylated state in hPDI

The stability of the *S*-nitrosylated state will have an effect on its impact on PDI function. The mononitrosylated active site appears to be rapidly converted to the disulfide state (Figs. 1-2), but what about the dinitrosylated active site or the C343 nitrosylated state?

The dinitrosylated state of the active site of the isolated **a** domain formed from either SNOC or GSNO reached a peak after 3 min of reaction and steadily decreased thereafter (Fig. 2). This gain and decay could be fitted to a sequential reaction (Fig. 5A). Both fitted well with rate constants for the formation of the dinitrosylated species of 97 ± 10 $M^{-1}s^{-1}$ and 47 ± 3 $M^{-1}s^{-1}$ for the SNOC and GSNO derived species respectively (Fig 5B ; equivalent to pseudo first order rate constants of 2.9 and 1.4 min^{-1}) . These are consistent with the rate of loss of the reduced species. The loss of the dinitrosylated species was much slower, with apparent first order rate constants of 0.0082 ± 0.0013 min^{-1} and 0.014 ± 0.001 min^{-1}. While this could represent a spontaneous breakdown of the dinitrosylated species the difference in the rate of loss of this species (Fig. 5B) and the concomitant appearance of the active site disulfide (Fig. 2), suggests a mechanism based on the reaction of the low level amounts of cysteine and glutathione present in solution from the nitrosylation event (Fig. 5C). No transient mixed disulfide states between PDI and the low molecular weight thiol species were observed.

To further examine if the active site dinitrosylated states and the C343 nitrosylated

state are stable in the presence of GSH, reduced hPDI was reacted with SNOC or GSNO for an hour and then treated for 15 min with near physiological concentrations of GSH or a buffer control. Treatment with GSH resulted in the complete disappearance of the dinitrosylated active site species, but not the C343 nitrosylated state (Fig. 5D).

3.6 The *S*-nitrosylation of PDI in SH-SY5Y cells

Together this *in vitro* data suggests that the physiological effects of *S*-nitrosylation of PDI arise from *S*-nitrosylation of C343 and that *S*-nitrosylated C343 is stable in the presence of GSH.

To confirm that this effect is seen *in vivo*, SH-SY5Y cells were treated with SNOC for 30 min in the HBSS buffered with HEPES then the media replaced, and the cells incubated in FBS free culture medium for 24 h. *S*-nitrosylation of PDI was observed after the SNOC treatment and *S*-nitrosylated PDI was still detected 24 h after removing SNOC (Fig 6A), suggesting that the *S*-nitrosylation could not be rapidly reduced by endogenous reductants such as GSH.

We hypothesized that the primary site for *S*-nitrosylation of PDI *in vivo* would be C343. To examine this we transfected SH-SY5Y cells with plasmids stably expressing either wild-type PDI or the C343S mutant. Both proteins were expressed to the same level (Fig. 6B). While wild-type PDI was *S*-nitrosylated, the level of *S*-nitrosylation of the C343S mutant was

substantially lower and only wild-type PDI of *S*-nitrosylation remained 24 h after removing SNOC (Fig. 6C). This matches the *in vitro* results that C343 in the **b'** domain is the primary site for *S*-nitrosylation of PDI.

4. Discussion

PDI is an essential enzyme for oxidative protein folding, catalysing the formation, breakage, and rearrangement of disulfide bonds in folding proteins (12, 33). In addition to its oxidoreductase activity, PDI also acts as a molecular chaperone for unfolded/misfolded proteins [9–11]. In some neurodegenerative disease patients, *S*-nitrosylated PDI accumulated in their brain [24,25]. However, to our knowledge the *S*-nitrosylation site in PDI has not been defined. Due to their high reactivity, the assumption is that the site is at one of the active sites. Here we show that while the active site cysteines of PDI are reactive towards various nitrosocompounds *S*-nitrosylation of the active site results in the net formation of an active site disulfide, unless the nitrocompound is in large excess so that both active site cysteines become *S*-nitrosylated at the same time. Active site *S*-nitrosylation, including active site dinitrosylation, is reversible by GSH as the active site is exposed and since glutathione is an endogenous substrate of PDI [15].

Here we identify that *in vitro* and *in vivo S*-nitrosylation of C343 in the **b'** domain of PDI occurs. *S*-nitrosylation of C343 is only slowly reversible by GSH. These results suggest that *S*-nitrosylation of C343 in PDI may be the causative effect results in the previously reported

physiological changes in neurodegerenative disease patients. Studying the *in vitro* effects of C343 nitrosylation on the function of PDI is problematic as C343 cannot be nitrosylated in the oxidized state of PDI and nitrosylation from the reduced state results in a mixture of species (e.g. Fig 1) which cannot be readily separate from each other.

While not involved in direct catalysis of thiol-disulfide exchange, the **b'** domain contains the primary substrate binding site of PDI [14,18,19]. Though C343 is not responsible for substrate binding [18], it is located below the binding site, suggesting that *S*-nitrosylation at this cysteine may modulate substrate binding affinity/specificity or interaction with Ero1 which uses the same site [40] or the formation of a complex with MTPα which also uses the same site [41].

While endogenous compounds, including PDI, could not reduce *S*-nitrosylated PDI C343 there is the possibility that flavonoid glycosides might. For example, neohesperidin, which is a flavonoid glycoside, alleviated $A\beta_{25–35}$-triggered generation of *S*-nitrosylated PDI in neuro cells [42] and rutin, another flavonoid glycoside with antioxidant activity could bind at the **b'** domain of PDI [43]. Together, these findings suggest that some flavonoids might be able to access the *S*-nitrosylated C343 and reduce it back to the free thiol. Furthermore, this suggests that flavonoids may be useful compounds for the development of new prevention and treatment for neurodegenerative diseases.

5. Conclusions

In this study, we identify that *in vitro* and *in vivo* *S*-nitrosylation of C343 in the **b'** domain of PDI occurs. Active site disulfide, dinitrosylated species, and mononitrosylated species were observed by the *S*-nitrosylation of reduced hPDI. Active site *S*-nitrosylation is reversible by GSH but *S*-nitrosylation of C343 is comparative stable both of *in vitro* and *in vivo*, suggesting that *S*-nitrosylation of C343 in PDI may be the causative effect on physiological changes in neurodegerenative disease patients. The results of our study provide a new insight into the proceeding neurodegeneration, and may be useful for the drug development for neurodegenerative diseases.

Declaration of interest

The authors report no conflicts of interest. The authors alone are responsible for the content and writing of this article.

Acknowledgements

We are most grateful to Dr. Ulrich Bergmann for assistance with the mass spectrometry. We would like to thank Biomedical Research Unit of Tohoku University Hospital (BRU) for technical support. This study was in part supported by the Uehara Memorial Foundation fellowships to J.O. and the Japan Society for the Promotion of Science (JSPS) KAKENHI grant

number 18H06099 and 19K21219 to J.O.

References

[1] J. Cummings, G. Lee, A. Ritter, M. Sabbagh, K. Zhong, Alzheimer's disease drug development pipeline: 2019, Alzheimer's Dement. Transl. Res. Clin. Interv. 5 (2019) 272–293. https://doi.org/10.1016/j.trci.2019.05.008.

[2] A. Elkouzi, V. Vedam-Mai, R.S. Eisinger, M.S. Okun, Emerging therapies in Parkinson disease — repurposed drugs and new approaches, Nat. Rev. Neurol. 15 (2019) 204–223. https://doi.org/10.1038/s41582-019-0155-7.

[3] M.K. Jaiswal, Riluzole and edaravone: A tale of two amyotrophic lateral sclerosis drugs, Med. Res. Rev. 39 (2019) 733–748. https://doi.org/10.1002/med.21528.

[4] C.A. Ross, M.A. Poirier, Protein aggregation and neurodegenerative disease, Nat. Med. 10 (2004) S10. https://doi.org/10.1038/nm1066.

[5] B.N. Dugger, D.W. Dickson, Pathology of neurodegenerative diseases, Cold Spring Harb. Perspect. Biol. 9 (2017) 1–22. https://doi.org/10.1101/cshperspect.a028035.

[6] B.N. Dugger, J.G. Hentz, C.H. Adler, M.N. Sabbagh, H.A. Shill, S. Jacobson, J.N. Caviness, C. Belden, E. Driver-Dunckley, K.J. Davis, L.I. Sue, T.G. Beach, Clinicopathological outcomes of prospectively followed normal elderly brain bank volunteers, J. Neuropathol. Exp. Neurol. 73 (2014) 244–252. https://doi.org/10.1097/NEN.0000000000000046.

[7] R. Frigerio, H. Fujishiro, T.B. Ahn, K.A. Josephs, D.M. Maraganore, A. DelleDonne, J.E. Parisi, K.J. Klos, B.F. Boeve, D.W. Dickson, J.E. Ahlskog, Incidental Lewy body

disease: Do some cases represent a preclinical stage of dementia with Lewy bodies?, Neurobiol. Aging. 32 (2011) 857–863. https://doi.org/10.1016/j.neurobiolaging.2009.05.019.

[8] V.G.H. Evidente, C.H. Adler, M.N. Sabbagh, D.J. Connor, J.G. Hentz, J.N. Caviness, L.I. Sue, T.G. Beach, Neuropathological findings of PSP in the elderly without clinical PSP: Possible incidental PSP?, Park. Relat. Disord. 17 (2011) 365–371. https://doi.org/10.1016/j.parkreldis.2011.02.017.

[9] J. Winter, P. Klappa, R.B. Freedman, H. Lilie, R. Rudolph, Catalytic activity and chaperone function of human protein-disulfide isomerase are required for the efficient refolding of proinsulin, J. Biol. Chem. 277 (2002) 310–317. https://doi.org/10.1074/jbc.M107832200.

[10] C. Wang, Protein Disulfide Isomerase Assists Protein Folding as Both an Isomerase and a Chaperone, Ann. N. Y. Acad. Sci. 864 (1998) 9–13.

[11] Y. Yao, Y.C. Zhou, C.C. Wang, Both the isomerase and chaperone activities of protein disulfide isomerase are required for the reactivation of reduced and denatured acidic phospholipase A 2, EMBO J. 16 (1997) 651–658. https://doi.org/10.1093/emboj/16.3.651.

[12] F. Hatahet, L.W. Ruddock, Protein disulfide isomerase: A critical evaluation of its function in disulfide bond formation, Antioxidants Redox Signal. 11 (2009) 2807–

2850. https://doi.org/10.1089/ars.2009.2466.

[13] L. Ellgaard, L.W. Ruddock, The human protein disulphide isomerase family: Substrate interactions and functional properties, EMBO Rep. 6 (2005) 28–32. https://doi.org/10.1038/sj.embor.7400311.

[14] C. Wang, W. Li, J. Ren, J. Fang, H. Ke, W. Gong, W. Feng, C.C. Wang, Structural insights into the redox-regulated dynamic conformations of human protein disulfide isomerase, Antioxidants Redox Signal. 19 (2013) 44–53. https://doi.org/10.1089/ars.2012.4630.

[15] A.K. Lappi, L.W. Ruddock, Reexamination of the role of interplay between glutathione and protein disulfide isomerase, J. Mol. Biol. 409 (2011) 238–249. https://doi.org/10.1016/j.jmb.2011.03.024.

[16] H.I. Alanen, K.E.H. Salo, A. Pirneskoski, L.W. Ruddock, pH dependence of the peptide thiol-disulfide oxidase activity of six members of the human protein bisulfide isomerase family, Antioxidants Redox Signal. 8 (2006) 283–291. https://doi.org/10.1089/ars.2006.8.283.

[17] L.W. Ruddock, T.R. Hirst, R.B. Freedman, PH-dependence of the dithiol-oxidizing activity of DsbA (a periplasmic protein thiol:disulphide oxidoreductase) and protein disulphide-isomerase: Studies with a novel simple peptide substrate, Biochem. J. 315 (1996) 1001–1005. https://doi.org/10.1042/bj3151001.

[18] P. Klappa, L.W. Ruddock, N.J. Darby, R.B. Freedman, The b' domain provides the principal peptide-binding site of protein disulfide isomerase but all domains contribute to binding of misfolded proteins, EMBO J. 17 (1998) 927–935. https://doi.org/10.1093/emboj/17.4.927.

[19] A. Pirneskoski, P. Klappa, M. Lobell, R.A. Williamson, L. Byrne, H.I. Alanen, K.E.H. Salo, K.I. Kivirikko, R.B. Freedman, L.W. Ruddock, Molecular Characterization of the Principal Substrate Binding Site of the Ubiquitous Folding Catalyst Protein Disulfide Isomerase, J. Biol. Chem. 279 (2004) 10374–10381. https://doi.org/10.1074/jbc.M312193200.

[20] U. Woehlbier, A. Colombo, M.J. Saaranen, V. Pérez, J. Ojeda, F.J. Bustos, C.I. Andreu, M. Torres, V. Valenzuela, D.B. Medinas, P. Rozas, R.L. Vidal, R. Lopez-Gonzalez, J. Salameh, S. Fernandez-Collemann, N. Muñoz, S. Matus, R. Armisen, A. Sagredo, K. Palma, T. Irrazabal, S. Almeida, P. Gonzalez-Perez, M. Campero, F. Gao, P. Henny, B. Zundert, L.W. Ruddock, M.L. Concha, J.P. Henriquez, R.H. Brown, C. Hetz, ALS -linked protein disulfide isomerase variants cause motor dysfunction , EMBO J. 35 (2016) 845–865. https://doi.org/10.15252/embj.201592224.

[21] Q. Yang, Z.B. Guo, Polymorphisms in protein disulfide isomerase are associated with sporadic amyotrophic lateral sclerosis in the Chinese Han population, Int. J. Neurosci. 126 (2016) 607–611. https://doi.org/10.3109/00207454.2015.1050098.

[22] P. Gonzalez-Perez, U. Woehlbier, R.J. Chian, P. Sapp, G.A. Rouleau, C.S. Leblond, H. Daoud, P.A. Dion, J.E. Landers, C. Hetz, R.H. Brown, Identification of rare protein disulfide isomerase gene variants in amyotrophic lateral sclerosis patients, Gene. 566 (2015) 158–165. https://doi.org/10.1016/j.gene.2015.04.035.

[23] C.T. Kwok, A.G. Morris, J. Frampton, B. Smith, C.E. Shaw, J. De Belleroche, Association studies indicate that protein disulfide isomerase is a risk factor in amyotrophic lateral sclerosis, Free Radic. Biol. Med. 58 (2013) 81–86. https://doi.org/10.1016/j.freeradbiomed.2013.01.001.

[24] T. Uehara, T. Nakamura, D. Yao, Z.Q. Shi, Z. Gu, Y. Ma, E. Masliah, Y. Nomura, S.A. Lipton, S-Nitrosylated protein-disulphide isomerase links protein misfolding to neurodegeneration, Nature. 441 (2006) 513–517. https://doi.org/10.1038/nature04782.

[25] A.K. Walker, M.A. Farg, C.R. Bye, C.A. McLean, M.K. Horne, J.D. Atkin, Protein disulphide isomerase protects against protein aggregation and is S-nitrosylated in amyotrophic lateral sclerosis, Brain. 133 (2010) 105–116. https://doi.org/10.1093/brain/awp267.

[26] K. Vuori, R. Myllyla, T. Pihlajaniemi, K.I. Kivirikkos, Mutagenesis of Human Protein Disulfide Isomerase in Escherichia coli, J. Biol. Chem. 267 (1992) 7211–7214.

[27] A. Martínez-Ruiz, S. Lamas, Signalling by NO-induced protein S-nitrosylation and S-glutathionylation: Convergences and divergences, Cardiovasc. Res. 75 (2007) 220–

228. https://doi.org/10.1016/j.cardiores.2007.03.016.

[28] T. W.Hart, Some observations concerning the S-nitroso and S-phenylsulphonyl derivatives of L-cysteine and glutathione, Tetrahedron Lett. 26 (1985) 2013–2016. https://doi.org/10.1016/S0040-4039(00)98368-0.

[29] N. Watanabe, N. Ryuman, T. Arai, S-Nitrosation of cellular proteins by no donors in rat embryonic fibroblast 3Y1 cells: Factors affecting S-nitrosation, Oxid. Med. Cell. Longev. 2011 (2011). https://doi.org/10.1155/2011/450317.

[30] N.C. Onukwue, Scholarship at UWindsor Structure-function relationship in S-nitrosoglutathione reductase and the development of fluorogenic pseudo-substrates, (2019).

[31] S.I. Hashemy, A. Holmgren, Regulation of the catalytic activity and structure of human thioredoxin 1 via oxidation and S-nitrosylation of cysteine residues, J. Biol. Chem. 283 (2008) 21890–21898. https://doi.org/10.1074/jbc.M801047200.

[32] S.I. Hashemy, C. Johansson, C. Berndt, C.H. Lillig, A. Holmgren, Oxidation and S-nitrosylation of cysteines in human cytosolic and mitochondrial glutaredoxins: Effects on structure and activity, J. Biol. Chem. 282 (2007) 14428–14436. https://doi.org/10.1074/jbc.M700927200.

[33] H.I. Alanen, K.E.H. Salo, M. Pekkala, H.M. Siekkinen, A. Pirneskoski, L.W. Ruddock, Defining the Domain Boundaries of the Human Protein Disulfide Isomerases,

Antioxid. Redox Signal. 5 (2003) 367–374.

[34] A. Gaciarz, J. Veijola, Y. Uchida, M.J. Saaranen, C. Wang, S. Hörkkö, L.W. Ruddock, Systematic screening of soluble expression of antibody fragments in the cytoplasm of E. coli, Microb. Cell Fact. 15 (2016) 1–10. https://doi.org/10.1186/s12934-016-0419-5.

[35] M.J. Saaranen, A.R. Karala, A.K. Lappi, L.W. Ruddock, The role of Dehydroascorbate in disulfide bond formation, Antioxidants Redox Signal. 12 (2010) 15–25. https://doi.org/10.1089/ars.2009.2674.

[36] R. Sengupta, T.R. Billiar, J.L. Atkins, V.E. Kagan, D.A. Stoyanovsky, Nitric oxide and dihydrolipoic acid modulate the activity of caspase 3 in HepG2 cells, FEBS Lett. 583 (2009) 3525–3530. https://doi.org/10.1016/j.febslet.2009.10.016.

[37] G. Fedoseev, S. Ioppolo, T. Lamberts, J. Zhen, H. Cuppen, H. Linnartz, Efficient Surface Formation Route of Interstellar Hydroxylamine Through NO Hydrogenation. II. The Multilayer Regime in Interstellar Relevant Ices, J. Chem. Phys. 137 (2012) 054714. https://doi.org/10.1063/1.4738893.

[38] C. Wang, J. Yu, L. Huo, L. Wang, W. Feng, C.C. Wang, Human protein-disulfide isomerase is a redox-regulated chaperone activated by oxidation of domain a′, J. Biol. Chem. 287 (2012) 1139–1149. https://doi.org/10.1074/jbc.M111.303149.

[39] A. Delaunay-Moisan, A. Ponsero, M.B. Toledano, Reexamining the Function of Glutathione in Oxidative Protein Folding and Secretion, Antioxidants Redox Signal. 27

(2017) 1178–1199. https://doi.org/10.1089/ars.2017.7148.

[40] A. Moilanen, L.W. Ruddock, Non-native proteins inhibit the ER oxidoreductin 1 (Ero1)-protein disulfide isomerase relay when protein folding capacity is exceeded., J. Biol. Chem. 1 (2020) 1–20. https://doi.org/10.1074/jbc.RA119.011766.

[41] E.I. Biterova, M.N. Isupov, R.M. Keegan, A.A. Lebedev, A.A. Sohail, I. Liaqat, H.I. Alanen, L.W. Ruddock, The crystal structure of human microsomal triglyceride transfer protein, Proc. Natl. Acad. Sci. U. S. A. 116 (2019) 17251–17260. https://doi.org/10.1073/pnas.1903029116.

[42] J. Wang, Y. Yuan, P. Zhang, H. Zhang, X. Liu, Y. Zhang, Neohesperidin Prevents Aβ25–35-Induced Apoptosis in Primary Cultured Hippocampal Neurons by Blocking the S-Nitrosylation of Protein-Disulphide Isomerase, Neurochem. Res. 43 (2018) 1736–1744. https://doi.org/10.1007/s11064-018-2589-5.

[43] L. Lin, S. Gopal, A. Sharda, F. Passam, S.R. Bowley, J. Stopa, G. Xue, C. Yuan, B.C. Furie, R. Flaumenhaft, M. Huang, B. Furie, Quercetin-3-rutinoside Inhibits Protein Disulfide Isomerase by Binding to Its b′x Domain, J. Biol. Chem. 290 (2015) 23543–23552. https://doi.org/10.1074/jbc.M115.666180.

Figure Legends

Fig. 1 Time course of the reaction hPDI wild type with SNOC and GSNO

(A) Domain structure of hPDI. (B-C) The reaction of reduced wild-type PDI with 500 μM SNOC (B) or GSNO (C) was followed as a function of time by ESI-MS and the relative proportion of the products calculated. (D) The predicted oxidation scheme of reduced hPDI by a *S*-nitrosocompound.

Fig. 2 Time course of the reaction hPDI **a** domain with SNOC and GSNO

(A-B) The reaction hPDI **a** domain with 500 μM SNOC (B) or GSNO (C) was followed as a function of time by ESI-MS and the relative proportion of the products calculated. (C) The predicted production scheme of dinitrosylated hPDI **a** domain by *S*-nitrosocompound. (D-E) The reaction hPDI **a** domain C56S mutant with 500 μM SNOC (E) or GSNO (E) was followed as a function of time by ESI-MS and the relative proportion of the products calculated.

Fig. 3 Time course of the reaction hPDI wild type with SNO-EtOH

hPDI was reacted with 500μM SNO-EtOH for the designated time and the relative proportion of the products at each time point calculated.

Fig. 4 Time course of the reaction hPDI cysteine mutants with SNOC and GSNO

(A-F) PDI mutants were reacted with SNOC or GSNO for the designated time and the relative proportion of the products at each time point determined by ESI-MS. (A) The reaction hPDI

C312A mutant with 500 μM SNOC. (B) The reaction hPDI C343A mutant with 500 μM SNOC. (C) The reaction hPDI C312A/C343S mutant with 500 μM SNOC. (D) The reaction hPDI C312A mutant with 500 μM GSNO. (E) The reaction hPDI C343A mutant with 500 μM GSNO. (F) The reaction hPDI C312A/C343S mutant with 500 μM GSNO.

Fig. 5 The stability of mononitrosylated and dinitrosylated species of PDI.

(A) The reaction scheme of formation and breakdown of the dinitrosylated species by the reaction with excess *S*-nitrosocompound. (B) The time course change of the dinitrosylated species from the reaction of PDI **a** domain with 500 μM SNOC and GSNO. (C) The mechanistic scheme of formation and breakdown scheme of the dinitrosylated species by the reaction with excess *S*-nitrosocompound. (D) The effect of GSH on the *S*-nitrosylated hPDI produced by the reaction with *S*-nitrosocompounds. Calculated molecular weight of each species is as follows: 2 S-S bond no NO; 55865, 2 S-S bond 1 NO; 55769, 1 S-S bond 2 NO; 55925, no NO; 56369, 1 NO; 56273, 2 NO; 56177.

Fig. 6 *S*-nitrosylation of PDI in SH-SY5Y cells

(A) The *S*-nitrosylation of PDI by the treatment of 100 μM SNOC in SH-SY5Y. (B) The protein expression level of PDI after the transfection of plasmids containing EGFP, human PDI wild type and PDI C343S. (C) The *S*-nitrosylation of PDI by the treatment of 100 μM SNOC in PDI-

overexpressed SH-SY5Y cells

Fig. S1 The reaction conditions of synthesis of *S*-nitrosocompounds.

(A) The scheme of the reaction. (B) The time dependences of the yields of synthesized *S*-nitrosocompounds. (C) The concentration dependences of the yields of synthesized *S*-nitrosocompounds. (D) Stabilities of synthesized *S*-nitrosocompounds. The yields were calculated spectrometrically using extinction coefficients ε_{338} = 900$M^{-1}cm^{-1}$, ε_{335} = 920$M^{-1}cm^{-1}$ and ε_{335} = 920$M^{-1}cm^{-1}$ for SNOC, GSNO and SNO-EtOH, respectively.

Fig. S2 Time course of the reaction hPDI with a lower concentration of SNOC and GSNO.

(A-B) The reaction hPDI wild type with 100 μM SNOC (A) or GSNO (B) was followed by ESI-MS and the relative proportion of products as a function of time plotted. (C-D) The formation of the dinitrosylated species by the reaction with different concentrations of SNOC (C) or GSNO (D).

1 Figure 1

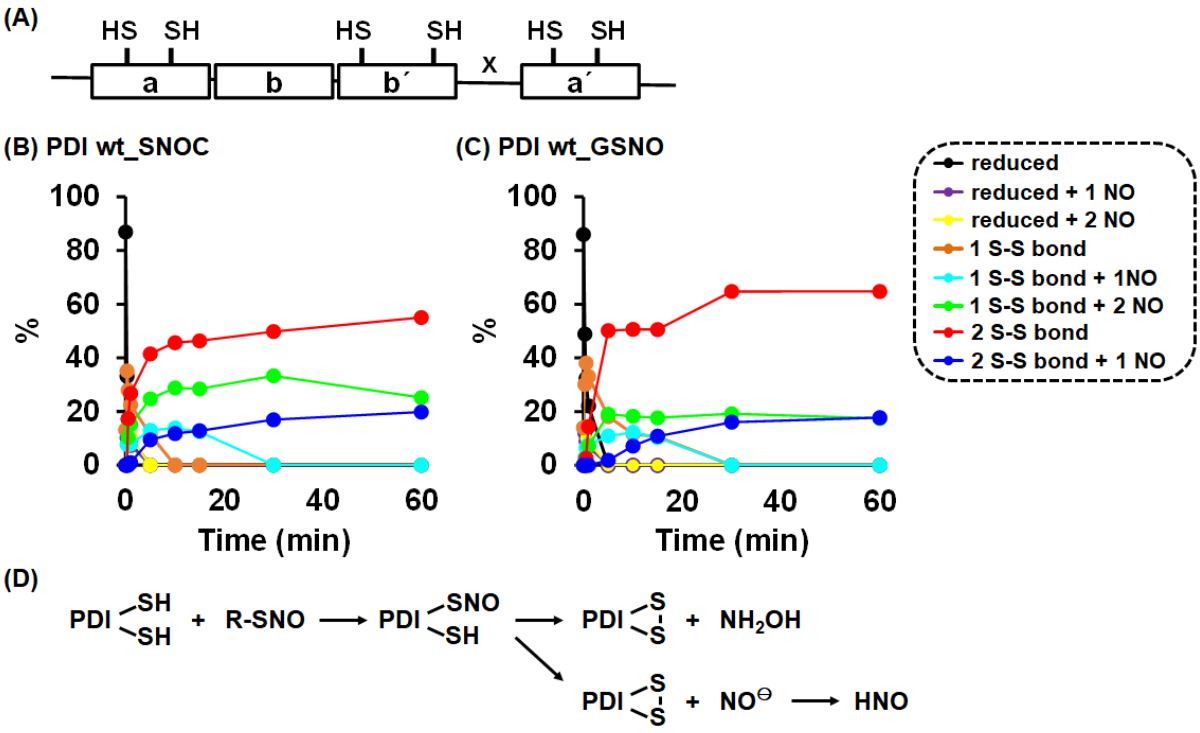
(A)
HS SH HS SH HS SH
a b b´ x a´
(B) PDI wt_SNOC
(C) PDI wt_GSNO
%
Time (min)
reduced
reduced + 1 NO
reduced + 2 NO
1 S-S bond
1 S-S bond + 1NO
1 S-S bond + 2 NO
2 S-S bond
2 S-S bond + 1 NO
(D)
PDI SH SH + R-SNO → PDI SNO SH → PDI S S + NH2OH
PDI S S + NO⊖ → HNO

2

3

Figure 2

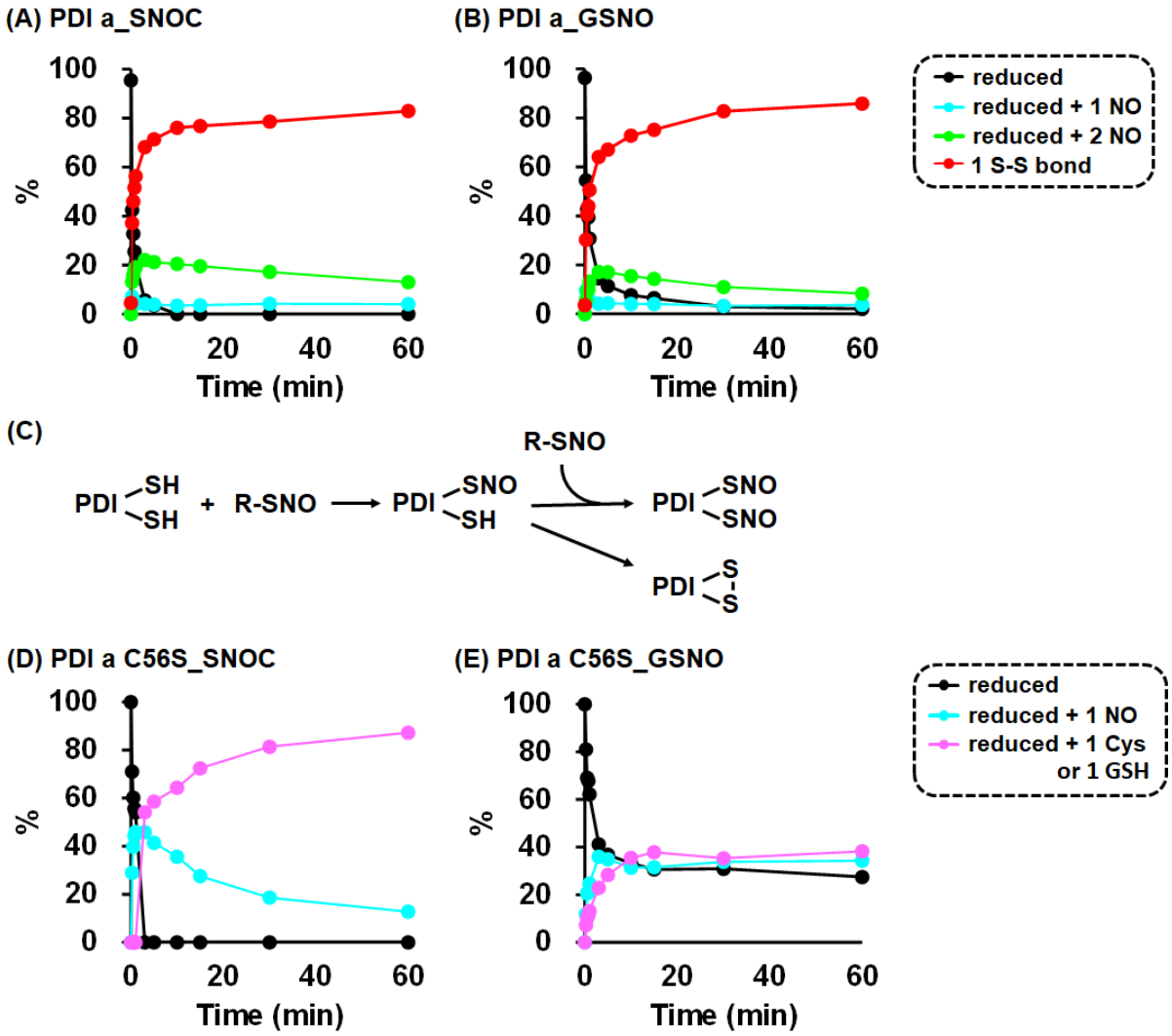
(A) PDI a_SNOC
(B) PDI a_GSNO
100
80
60
40
20
0
%
0
20
40
60
Time (min)
reduced
reduced + 1 NO
reduced + 2 NO
1 S-S bond
(C)
PDI SH SH + R-SNO → PDI SNO SH
R-SNO
PDI SNO SNO
PDI S S
(D) PDI a C56S_SNOC
(E) PDI a C56S_GSNO
reduced
reduced + 1 NO
reduced + 1 Cys or 1 GSH

Figure 3

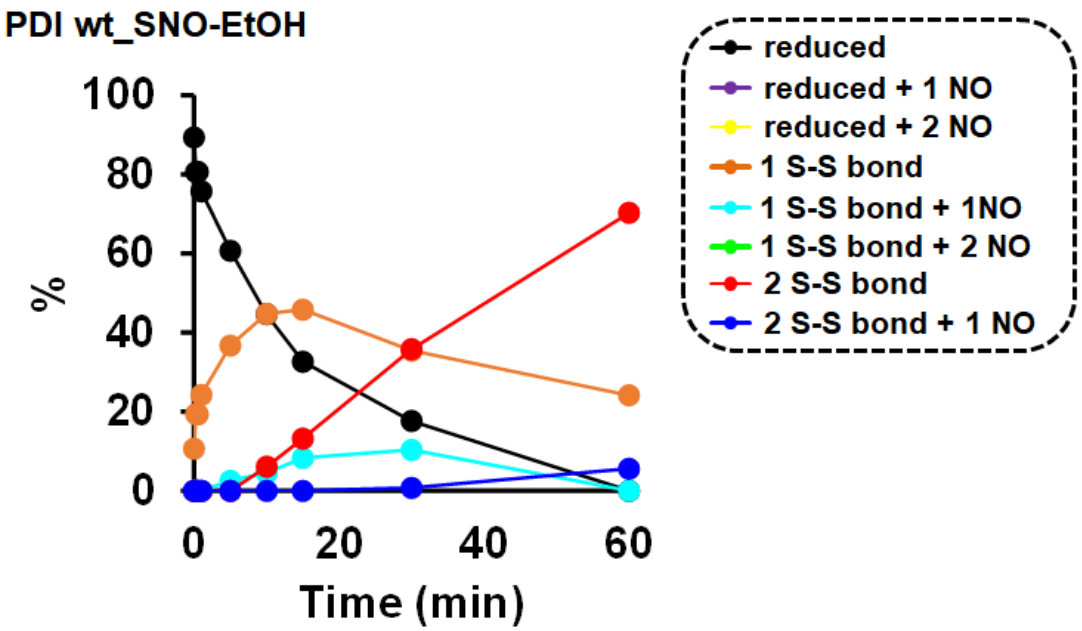
PDI wt_SNO-EtOH
100
80
60
40
20
0
%
0
20
40
60
Time (min)
reduced
reduced + 1 NO
reduced + 2 NO
1 S-S bond
1 S-S bond + 1NO
1 S-S bond + 2 NO
2 S-S bond
2 S-S bond + 1 NO

Figure 4

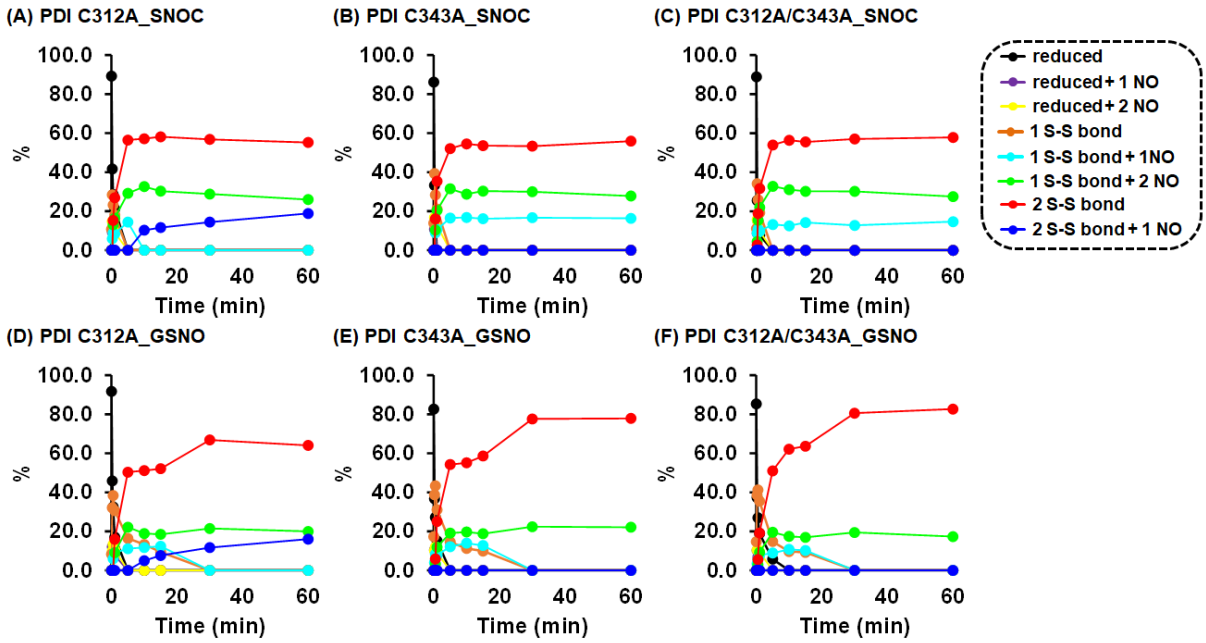
(A) PDI C312A_SNOC
(B) PDI C343A_SNOC
(C) PDI C312A/C343A_SNOC
(D) PDI C312A_GSNO
(E) PDI C343A_GSNO
(F) PDI C312A/C343A_GSNO
%
Time (min)
reduced
reduced + 1 NO
reduced + 2 NO
1 S-S bond
1 S-S bond + 1NO
1 S-S bond + 2 NO
2 S-S bond
2 S-S bond + 1 NO

Figure 5

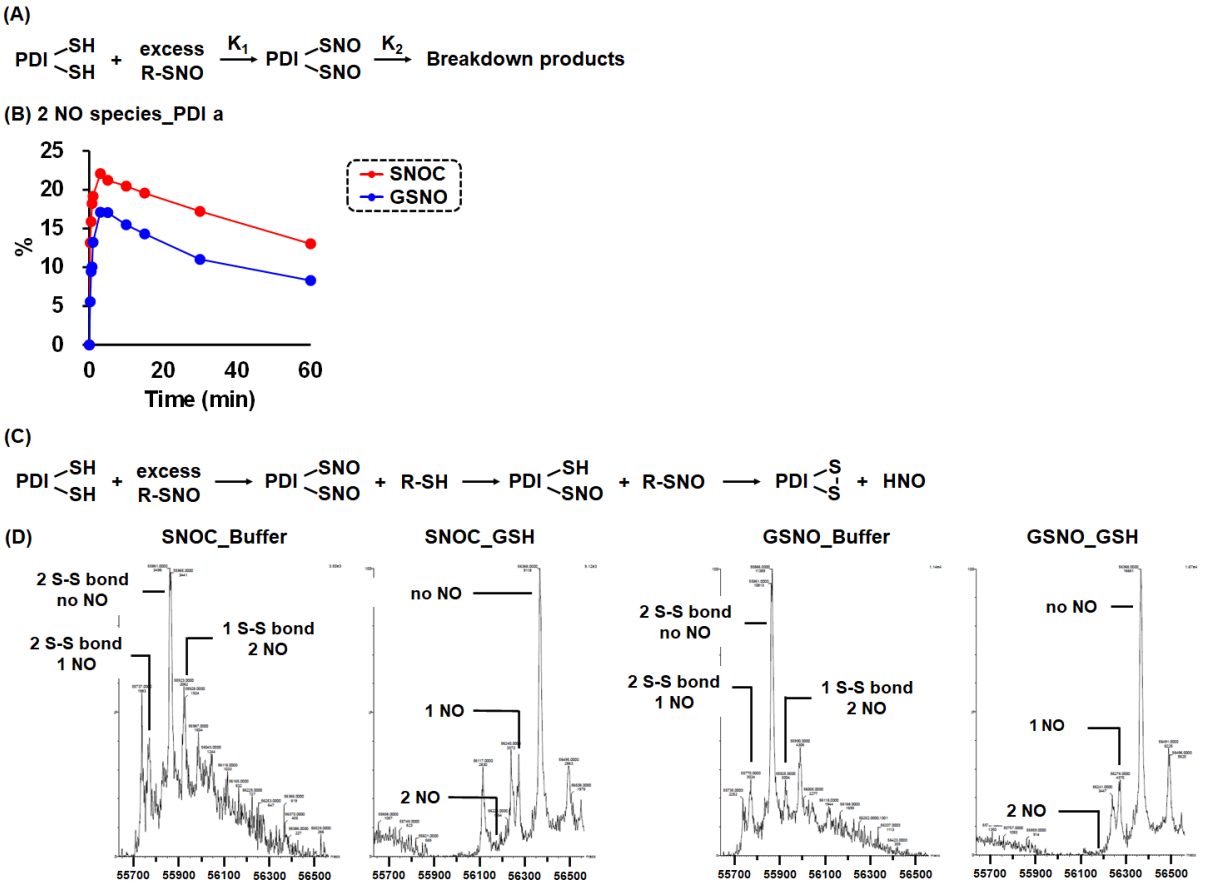
(A)
PDI SH SH + excess R-SNO K1 PDI SNO SNO K2 Breakdown products
(B) 2 NO species_PDI a
25
20
15
10
5
0
%
0
20
40
60
Time (min)
SNOC
GSNO
(C)
PDI SH SH + excess R-SNO PDI SNO SNO + R-SH PDI SH SNO + R-SNO PDI S S + HNO
(D)
SNOC_Buffer
SNOC_GSH
GSNO_Buffer
GSNO_GSH
2 S-S bond no NO
2 S-S bond 1 NO
1 S-S bond 2 NO
no NO
1 NO
2 NO
55700
55900
56100
56300
56500

1 Figure 6

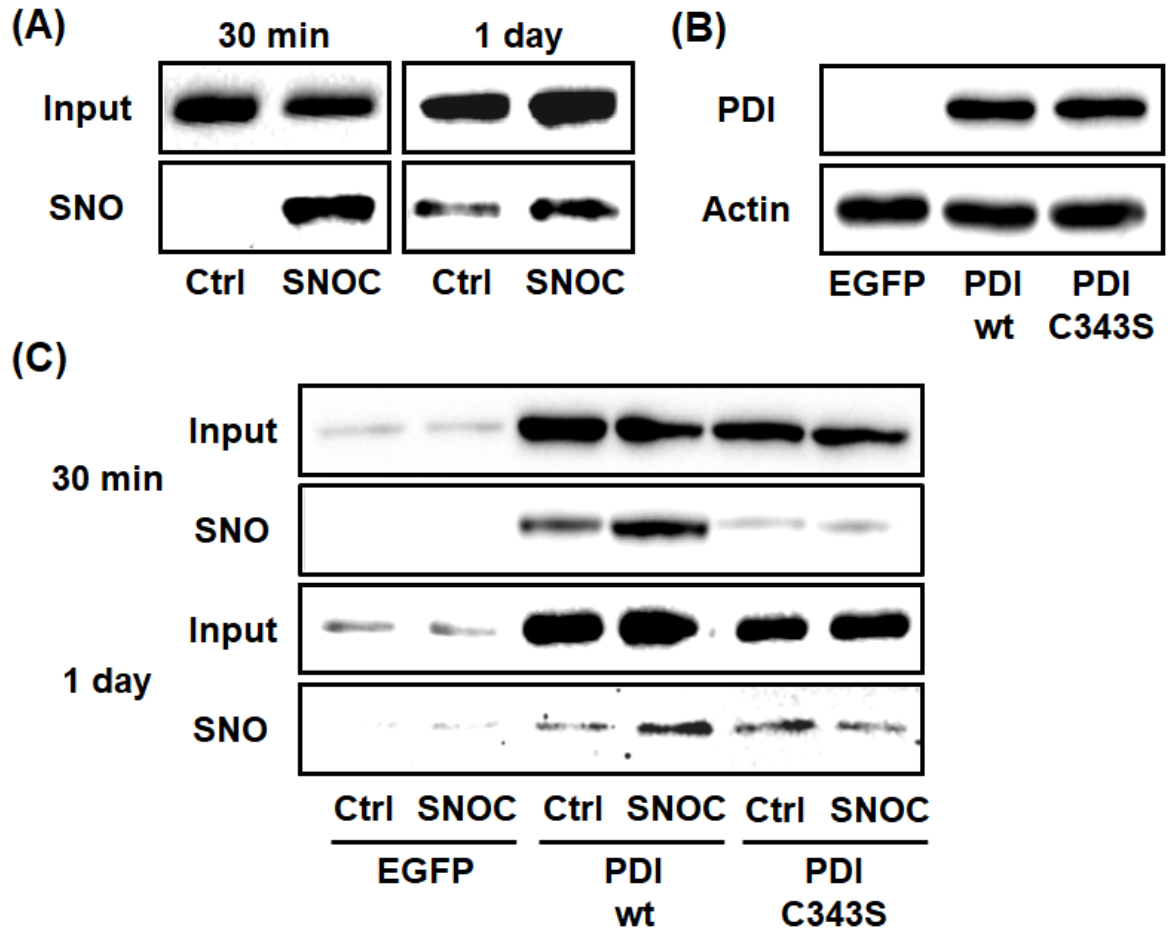
(A)
30 min
1 day
Input
SNO
Ctrl
SNOC
Ctrl
SNOC
(B)
PDI
Actin
EGFP
PDI wt
PDI C343S
(C)
30 min
Input
SNO
1 day
Input
SNO
Ctrl
SNOC
Ctrl
SNOC
Ctrl
SNOC
EGFP
PDI wt
PDI C343S

2

3

1 Figure S1

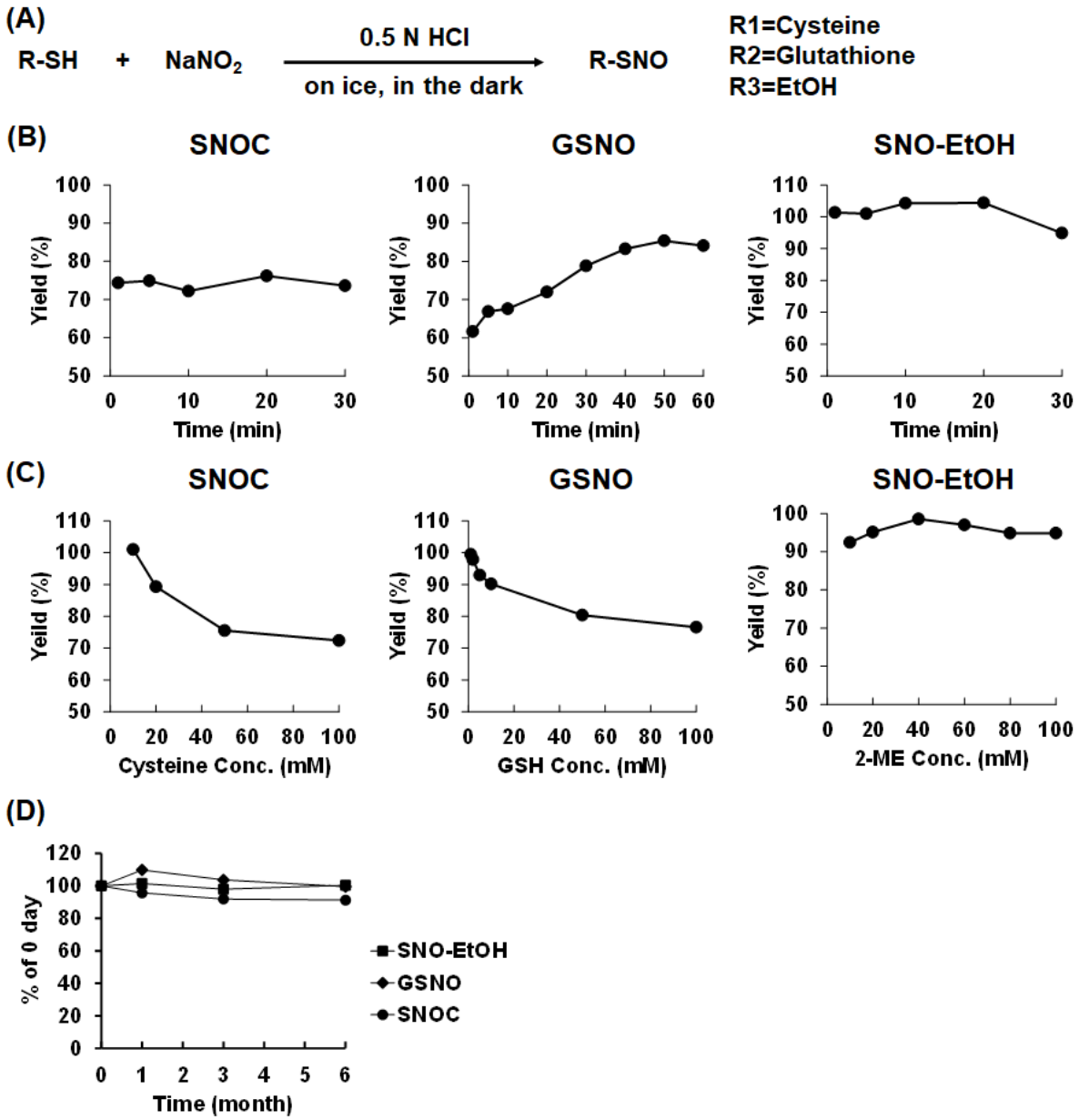

2

3

Figure S2

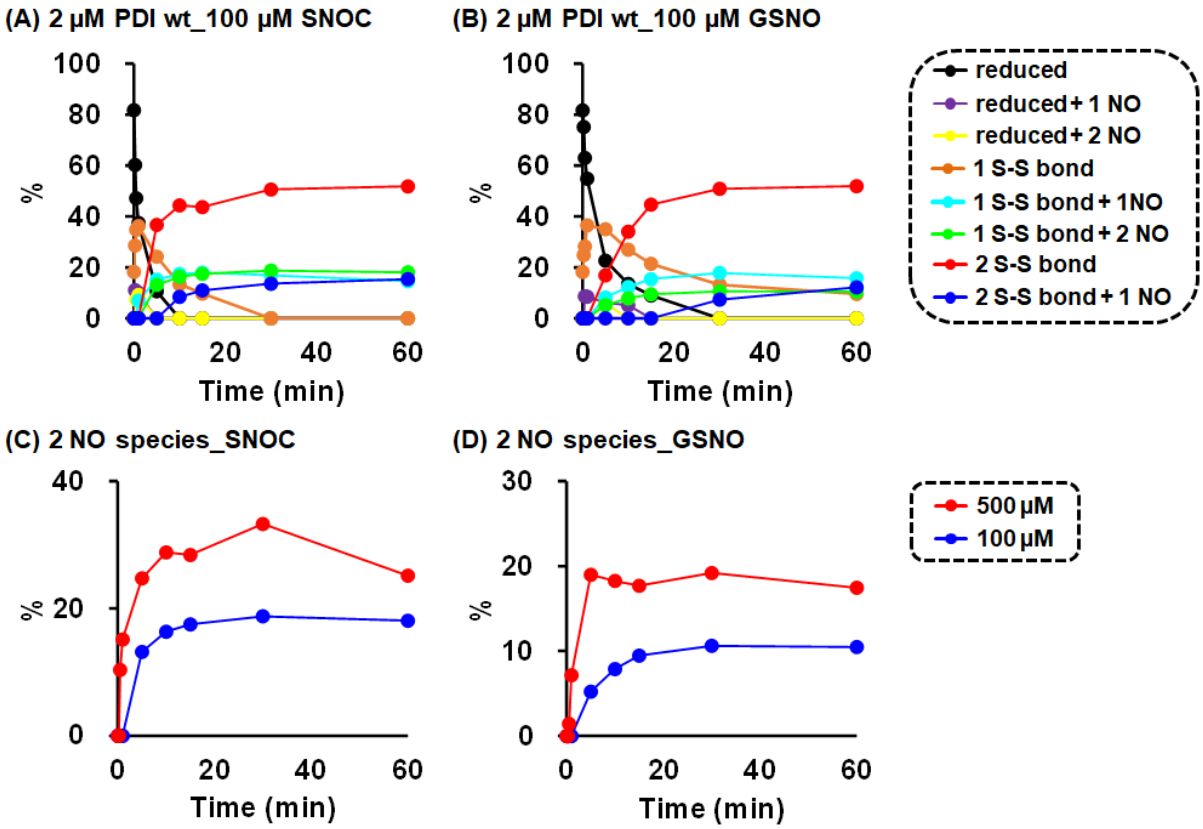
(A) 2 μM PDI wt_100 μM SNOC
(B) 2 μM PDI wt_100 μM GSNO
reduced
reduced + 1 NO
reduced + 2 NO
1 S-S bond
1 S-S bond + 1NO
1 S-S bond + 2 NO
2 S-S bond
2 S-S bond + 1 NO
%
Time (min)
(C) 2 NO species_SNOC
(D) 2 NO species_GSNO
500 μM
100 μM